



## Analyzing energy performance and assessing dry moisture content of briquettes through numerical investigations



Oluwaseyi O. Alabi <sup>a,b\*</sup>, Timothy A. Adeyi <sup>a</sup>, Sakiru K. Ekun <sup>a</sup>

<sup>a</sup>Department of Mechanical Engineering, Lead City University, Ibadan, Nigeria.

<sup>b</sup>Department of Mechanical Engineering, University of Ibadan, Nigeria.

\*Corresponding author Email: [alabi.oluwaseyi@lcu.edu.ng](mailto:alabi.oluwaseyi@lcu.edu.ng)

### HIGHLIGHTS

- Numerical analysis of briquette performance reveals potential energy savings via optimized moisture content.
- Findings suggest energy savings via optimization of moisture content in briquette production.
- Briquette moisture optimization could lead to improved efficiency and performance, aiding sustainable energy.

### ABSTRACT

This study presents a comprehensive numerical investigation into the energy evaluation and determination of dry moisture content of briquettes, a vital aspect of renewable energy production. Utilizing advanced computational fluid dynamics (CFD) modeling and simulations, we explored key parameters impacting briquette combustion, such as moisture content, size, density, and temperature profiles. The research demonstrates that these factors significantly influence combustion behavior, with the CFD model accurately predicting mass loss curves and burnout times. The process was completed in 10 minutes, reaching a temperature of 300K and yielding gases consisting of CO<sub>2</sub>, CO, and H<sub>2</sub>O, while the devolatilization front was assumed to be at 325K. The drying front was estimated to occur within the range of 303K to 310K. This knowledge is pivotal in optimizing briquettes as a sustainable energy source, ensuring efficient energy conversion, and reducing environmental impact. By integrating engineering principles, thermodynamics, and computational modeling, our interdisciplinary approach addresses complex challenges in renewable energy. The research findings underscore the importance of refining and validating these models to advance the understanding and utilization of briquettes as a clean and eco-friendly energy alternative. In a world increasingly prioritizing environmental sustainability and energy efficiency, this research aligns with broader efforts to transition towards cleaner and more sustainable energy sources, offering prospects for a greener and responsible energy future.

### ARTICLE INFO

**Handling editor:** Sattar Aljabair

#### Keywords:

Briquette Characterization  
CFD Modeling  
Combustion Parameters  
Sensible heat  
Sustainable Energy

## 1. Introduction

The urgency for alternative fuel sources has escalated within a society that places paramount importance on environmental sustainability and energy efficiency. Currently, fossil fuels, primarily consisting of coal, oil, and natural gas, fulfill a staggering 80% of the world's energy requirements [1]. Additionally, it was noted that, after coal and oil, raw biomass is the third most common source of energy worldwide [2]. The levels of greenhouse gases (GHGs) in the atmosphere have experienced a rapid escalation since the onset of the Industrial Revolution, and there exists a direct correlation between this surge and the combustion of fossil fuels. Consequently, a worldwide endeavor is underway to discover alternative energy sources with a reduced environmental impact [3]. Therefore, switching to renewable energy sources is necessary to lessen reliance on fossil fuels [4-6]. Using biomass briquettes as an alternative fuel source is a promising approach that has received more attention in recent years. Briquettes are compressed blocks of biomass or other organic materials that can replace traditional fossil fuels with a cleaner, more sustainable energy source. Briquettes are an essential alternative fuel source because they can lessen the negative effects of energy use on the environment, stop deforestation, and support sustainable development [7].

Biomass briquettes are often used as a renewable and low-carbon alternative to fossil fuels due to their low CO<sub>2</sub> emissions. They are a sustainable energy source that has the potential to help reduce our reliance on fossil fuels [8,9]. However, the efficient combustion of biomass briquettes remains the main issue. This is why a numerical simulation was chosen to optimize the biomass briquettes' burning characteristics [8,10]. As we further explore the realm of briquettes, it becomes clear that comprehending their energy assessment and moisture content is vital for their effective adoption and broad usage. Energy assessment enables us

to gauge the calorific value of briquettes, establishing their energy efficiency and suitability for various applications, spanning from residential heating to industrial operations. Conversely, analyzing moisture content is crucial for upholding the quality and consistency of briquettes. Elevated moisture levels can diminish combustion efficiency and heighten emissions, compromising the fundamental purpose of employing briquettes as an environmentally friendly alternative.

Numerical simulations are commonly utilized in experimental research concerning wind, solar, and fossil fuel energy due to their effectiveness and utility [11,12]. Utilizing computational fluid dynamics (CFD) simulations enables the exploration of numerous variables within the combustion process [13,14]. One advantage lies in their capacity to assess diverse operational scenarios and predict field values across the entire domain, even in regions where acquiring measurements in experimental tests could disrupt the system's operation. Much of the existing research has focused on predicting species concentrations, temperatures, and ignition rates by modeling biomass's combustion and gasification processes in zero-dimensional or one-dimensional beds, as reported in a review conducted by [15]. Researchers worldwide have developed numerous numerical models to examine the combustion of various biomass briquette boilers, along with the growing use of biomass briquette boilers. Naser et al. [16], researched intraparticle gradients, applying a porous medium approximation, and modeling fixed bed combustion.

Their study's findings confirm that using the porous medium approximation significantly influences the release of volatiles and moisture within the bed. Moreover, it also impacts the temperature profile when dealing with fuel beds composed of larger particles ( $>2$  cm). This modeling approach allows for examining the interplay between drying, pyrolysis, and coke combustion at various stages of the combustion process. Importantly, the results obtained from the model closely matched the experimental outcomes. In the context of a one-dimensional model, Mehrabian et al. [17] developed a thorough general model for biomass combustion, and three sets of experimental data were used to confirm the model's validity. In a study conducted by Plis and Wilk they examined the gasification of biomass with air in a fixed-bed boiler [18]. They developed a theoretical model grounded in equilibrium and thermodynamic principles within the gasification zone. The resulting syngas from the gasification process were subsequently introduced into the coal-burning zone of the boiler, where it was co-combusted with coal. The composition of the syngas is primarily influenced by factors such as the moisture content of the biomass and the air-to-fuel ratio used during gasification, with the type of biomass also playing a critical role.

To develop a robust model, Jacobo et al. [19] conducted simulations to replicate the steady operation of a biomass boiler and analyzed heat dynamics across different operational conditions. They validated the model's precision by comparing simulation outcomes with experimental results in two distinct scenarios [20]. This validation process yielded outstanding results when assessing the boiler's heat efficiency and pollutant emissions metrics. Porteiro introduced a dynamic framework [21] that swiftly evolved to encompass the modeling of processes, encompassing ignition, operation, and burnout, enabling real-time monitoring of the combustion process. While the literature contains various simulations for biomass molding boilers, there is a scarcity of 3D dynamic models tailored for boiler beds and the combustion of bed briquettes. Although some models related to particle pyrolysis exist [22], they do not fully address this specific aspect. Yuxiang et al. [23] introduced a wood combustion shrinkage model, which calculates the shrinkage rate by considering both constant density and the combustion process, reducing particle mass. Another more comprehensive model, considering changes in volatile fraction and porosity, was presented by Carter et al., [24]. Furthermore, Elkelawy et al. [25] devised a shrinkage model for individual particles that was verified, investigating its impact on species yields during pyrolysis across various Biot number ranges. Additionally, Weldekidan et al. [26], examined a particle shrinkage model that accounts for the degree of shrinkage caused by moisture, volatiles, and char conversion processes in particles and porosity.

This study involved conducting numerical simulations of bed combustion in a particular biomass briquette boiler using COMSOL Multiphysics. The accuracy of the model was validated through experimentation. This study introduces a novel approach, addressing significant gaps in our knowledge regarding wood briquettes as a crucial element in sustainable energy production, particularly in terms of their combustion behavior. Consequently, this research aims to enhance combustion processes and maximize energy yield from briquettes by employing a numerical modeling approach. By comprehending the sensible heat flow during wood briquette combustion, we anticipate achieving more efficient energy conversion and utilization, thus advancing the shift towards cleaner and more sustainable energy sources.

## 2. Methodology

### 2.1 Numerical model

The numerical method used in this study involved the finite element method (FEM), which is a technique for solving partial differential equations by breaking down the problem domain into a finite number of elements. The equations were solved using the COMSOL Multiphysics software package, which uses FEM to solve partial differential equations in physics and engineering problems. The details of the numerical modeling approach are outlined in the paper. The mesh created in this work has roughly 596,345 cells in total. The mesh generated was approximately 596,345 cells to balance accurately capturing detailed physical phenomena and maintaining reasonable computational efficiency. This cell count provided a robust representation of the system's geometry and behavior in our preliminary assessments. Figure 1(b) depicts a general perspective of the simulation's mesh and some specifics of the discretization used in the geometry's pertinent parts, Figure 1(a). Where the primary gradients were anticipated, finer mesh was used. In order to achieve grid independence, the grid size has been chosen so that various chosen quantities of the solution did not change noticeably as the grid's average element size decreased. The CFD models were based on an algorithm that uses numerical methods to simulate and analyze fluid flow, heat transfer, and other physical phenomena. As seen in Figure 2, the steady-state governing equations were solved using the SIMPLE algorithm, and the usual  $k$ -epsilon

model was used to account for the impact of turbulence on the mean flow. The discrete ordinate model was used to simulate radiant heat transfer.

## 2.2 Assumptions

The modeling of biomass combustion in the paper is based on the following assumptions:

- 1) The briquettes are assumed to have consistent material composition and density throughout the simulation.
- 2) The moisture content in the briquettes remains constant under varying conditions unless specifically addressed in the simulation.
- 3) The combustion behavior, including ignition temperature, burning rate, and heat release, remains consistent throughout the simulation.
- 4) The physical properties of the briquettes, such as thermal conductivity or specific heat, are assumed to be isotropic or uniform in all directions.
- 5) External factors such as environmental conditions (humidity, temperature) or mechanical stress are assumed to have a negligible impact on the properties being investigated.
- 6) It is assumed that no significant chemical changes occur within the briquettes during the simulated scenarios.
- 7) The simulation assumes steady-state conditions unless otherwise specified, disregarding transient effects.
- 8) The heating of the briquettes is assumed to be uniform, neglecting potential non-uniformities in heat distribution.
- 9) The simulation assumes ideal combustion without considering potential inefficiencies or by-products of combustion.
- 10) The material properties used in the simulation are assumed to be accurate and representative of the actual briquette material.

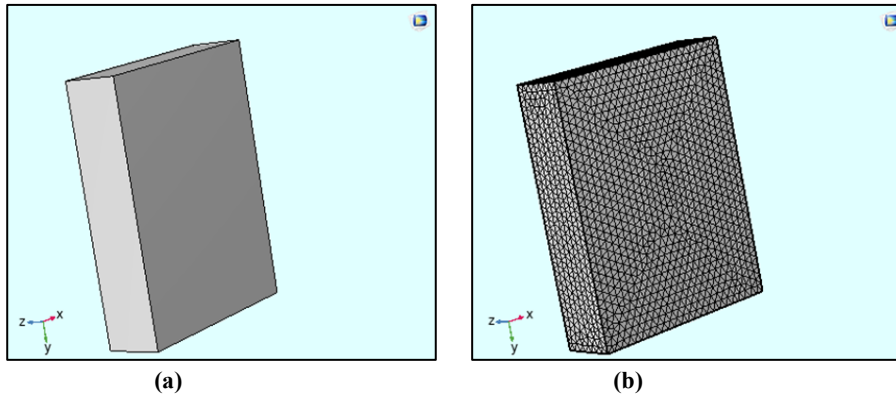


**Figure 1:** (a) Geometry model of briquet, (b) Mesh Generated

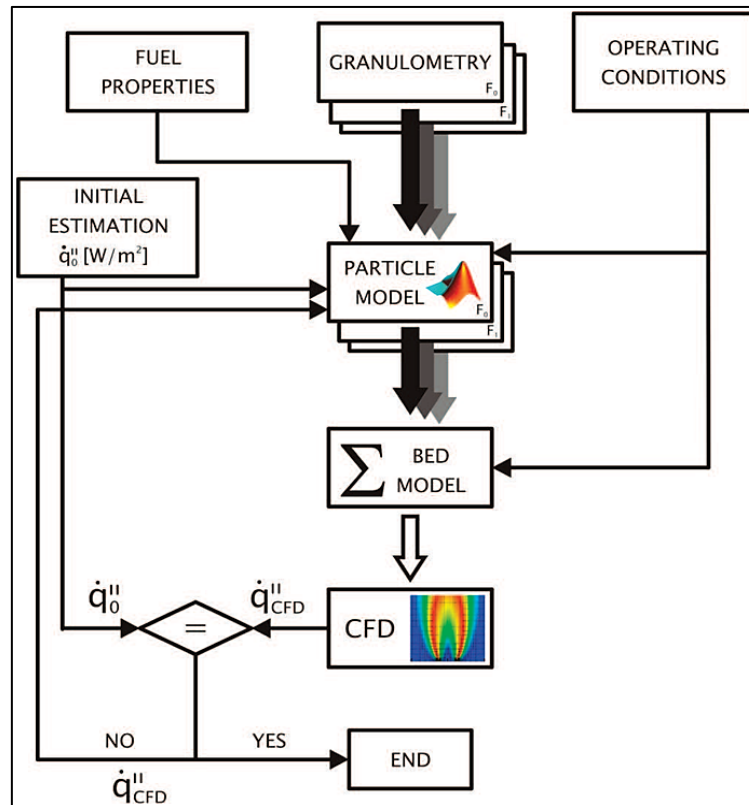


**Figure 2:** The algorithms employed in the CFD models [19]

### 2.3 Mathematical modelling

The characteristics of biomass fuel are purportedly shaped by their chemical composition and moisture content, with a fuel's vital component being its calorific value, as represented in Equation 1 by [13]

$$Q_c = (WT - e^1 - e^2e^3)/m \quad (1)$$

Where  $Q_c$  denotes the gross heat of combustion,  $T$  signifies the observed temperature rise,  $E$  represents the electrical equivalent of the calorimeter employed,  $e^1$  accounting for the heat generated when nitrogen from the trapped air in the bomb is combusted to form nitric acid,  $e^2$  reflecting the heat generated during the formation of sulfuric acid from the reaction involving sulfur dioxide, water, and oxygen,  $e^3$  standing for the heat generated by the combustion of the cotton thread and heating cord, and  $m$  indicating the mass of the sample. The transfer processes involved in biomass briquette combustion must adhere to the conservation equations for continuous, momentum, energy, and component transfer control. These Equations are as follows:

#### 1) Continuous equation

$$\frac{\partial \rho}{\partial t} + \frac{\partial}{\partial x_j} (\rho u_{g,j}) = 0 \quad (2)$$

where,  $\rho$  - the flow density;  $t$  - time;  $x_j - j$  - dimensional coordinate;  $u_{g,j}$  - velocity vector

#### 2) Momentum equation

$$\frac{\partial}{\partial t} (\rho H) + \frac{\partial}{\partial x_j} (\rho u_j H) = \frac{\partial}{\partial x_j} (\Gamma_h \frac{\partial}{\partial x_j} H) + \frac{\partial \rho}{\partial t} + S_h \quad (3)$$

where  $H$  is the total heat enthalpy of the fluid;  $u_j$  - velocity vector at the  $j$  - is the direction;  $\Gamma_h$  - heat transfer coefficient;  $\rho$  - fluid pressure; and  $S_h$  is the heat source and radiation heat transfer inside the fluid.

#### 3) Component transfer heat equation

It is feasible to see heat transfer, diffusive and convective mass transport within the particle, and the transient diffusive chemically reacting flow around it using a collection of conservation equations coupled with the proper initial and boundary conditions. This general differential Equation explains how the particle's mass, species, and energy are conserved.

$$\frac{\partial \rho Y_i}{\partial t} + \frac{\partial}{\partial x_j} (\rho u_j Y_i) = \frac{\partial}{\partial x_j} (\Gamma_i \frac{\partial}{\partial x_j} Y_i) + R_i + S_i \quad (4)$$

where,  $\Gamma_i$  - the component's mass transfer efficiency  $i$ ;  $Y_i$  - the mass fraction of component  $i$ ;  $R_i$  - the generation rate or consumption rate of component  $i$ ,  $S_i$  is the item of sources, including the production rate of component  $i$  introduced by the disperse item.

The CFD model employed here is a commercial one, which allows for seamless integration with external mathematical software and the inclusion of user-defined sub-models through C++ functions. Given the well-established fundamentals of CFD, this essay won't delve into their extensive explanation. The complete boiler model, encompassing the interplay between the bed and gas-phase models, was tackled through an iterative CFD procedure. A strong interdependence exists between the bed solution codes and the CFD models, as illustrated in Figure 2. Consequently, the boundary constraints imposed on the CFD model are determined by the outcomes of the fuel bed model. Once the CFD model has converged, its solution serves as the new boundary conditions for the bed model. This iterative process continues until both models converge simultaneously. The discrete phase model (DPM) trajectories are introduced into the CFD domain upon reaching the required aerodynamic size for suspension in the outflow gases. The boundary conditions for the CFD, derived from the bed model, encompass these particles' size, velocity, composition, and temperatures. The composition of each ejected particle can vary from freshly added wood to char, depending on its initial size.

The conservation equations governing continuity, momentum, energy, turbulence, chemical species, and soot are harnessed in the gas phase. These equations were solved using the built-in algorithm within the commercial CFD software. A second-order upwind approach was employed in all equations to address spatial discretization. Radiative heat transfer within the gas phase was represented using the discrete ordinate model (DOM), customized to interact with the solid phase. The realizable k-epsilon model was adopted to simulate turbulence, with special consideration given to the near-wall region. To account for the influence of the porous zone on gas flow, a momentum source term (Equation 5) was introduced, involving permeability coefficients and inertial losses determined through Equation 6 and 7, respectively [12]. These Equations consider the particle's sphericity (Equation 8) and equivalent diameter (Equation 9), as previously applied in similar studies.

$$S_{mom} = -\left(\frac{\mu}{\eta} v_\infty + \Upsilon \frac{1}{2} \rho_g v^2\right) \quad (5)$$

$$\eta = \frac{\psi^2 d_{eq}^2}{150} \frac{f_v^3}{(1-f_v)^2} \quad (6)$$

$$\Upsilon = \frac{3.5}{\psi d_{eq}} \frac{f_v^3}{(1-f_v)^2} \quad (7)$$

$$\psi = \frac{\pi^{1/3}(6V_p)^{2/3}}{A_p} \quad (8)$$

$$d_{eq} = D_{cil} \left( \frac{3L_{cil}}{2D_{cil}} \right)^{1/3} \quad (9)$$

## 2.4 Heat and mass transfer

Heat and mass transfer play pivotal roles in the combustion process. While the gas phase modeling is predominantly addressed by the commercial CFD software, it remains imperative to model heat and mass transfers within the solid phase, as well as the interactions between the two phases. Certain terms and variables that define heat transport are incorporated within the energy equation for the solid phase. Given wood's relatively low hardness, the thermal conductivity calculation in Equation (10) is grounded in the heat-electrical analogy, accounting for conduction through rectangular particles.

$$\dot{Q}_c = \frac{k_{s,eff} \cdot d_{eq}^2 \cdot \Delta T_s}{\lambda_e d_{eq}} = G \cdot \Delta T_s \quad (10)$$

$$G = \frac{G_s G_C}{G_s + G_C}, \quad G_s = \frac{1}{4} k_s \lambda_s \pi \cdot d_{eq}, \quad G_C = 2k_s \left( \frac{3F_n d_{eq}}{2E} \right)^{1/3} \quad (11)$$

A source term representing convective heat exchange is introduced within the solid energy equation (Equation 8). In contrast, the opposite is incorporated in the gas phase energy equation (Equation 12). To estimate the convective coefficient, Equation 13 is employed. The coefficients denoted as  $K_m^i$ , which influence the rate of char consumption, define the mass exchange. Their estimation is detailed in Equation 14, Equation 15 and 16 formulate the dimensionless numbers for Nusselt and Sherwood, respectively, [12] elucidating the mass and heat exchanges between the phases.

$$S_s^{conv} = -S_g^{conv} = hA_v(T_g - T_s) \quad (12)$$

$$h = \frac{Nu \cdot K_g}{d_{eq}} \quad (13)$$

$$K_m^i = \frac{Sh \cdot Di_i}{d_{eq}} \quad (14)$$

$$Nu = 2 + 1.1 \cdot Re^{0.6} \cdot Pr^{1/3} \quad (15)$$

$$Sh = 2 + 1.1 \cdot Re^{0.6} \cdot Sc^{1/3} \quad (16)$$

## 3. Results and discussion

Table 1 presents the data employed for modeling these briquettes. The model has been shown to predict the mass-loss curves' fundamental attributes successfully. The time needed for complete burnout of different particles varies depending on their initial moisture content, size, and density, falling within the range of 300 seconds to 600 seconds, consistent with both model predictions and experimental findings.

**Table 1:** Parameters and kinetic data are essential for simulating the behavior of briquettes

Parameter	Value
<b>Real density (kg.m<sup>-3</sup>)</b>	
Moisture	1000
Dry wood	1511
Char	1898
<b>Thermal Conductivity (W.m<sup>-1</sup>K<sup>-1</sup>)</b>	
Moisture	0.62
Dry wood	0.190
Gas	0.030
Char	0.10
<b>Specific heat (J.Kg<sup>-1</sup>K<sup>-1</sup>)</b>	
Moisture	4220
Dry wood	1420
Gas	1100
Char	1301
Evaporation heat of reaction (kJ/kg)	-3010

In the context of modeling single-briquet biomass combustion, the entire process was completed in a span of 10 minutes, reaching a temperature of 300 K and yielding gases consisting of CO<sub>2</sub>, CO, and H<sub>2</sub>O. Notably, as depicted in Figure 3, the initial stage involved rapid evaporation of free water from the briquet upon contact with hot air, which occurred around t=5 minutes. Subsequently, significant production of H<sub>2</sub>O and CO<sub>2</sub> commenced as the briquet temperature continued to rise at times 6, 7, 8,



9, and 10 minutes as shown in Figure 4. This was primarily attributed to removing flammable, volatile gases from the surface of the biomass pellets, which subsequently came into contact with oxygen, leading to exothermic chemical reactions. By  $t=10$  minutes, some volatiles on the top of the single-pellet biomass had burned, but more importantly, combustion had penetrated deeper into the briquette.

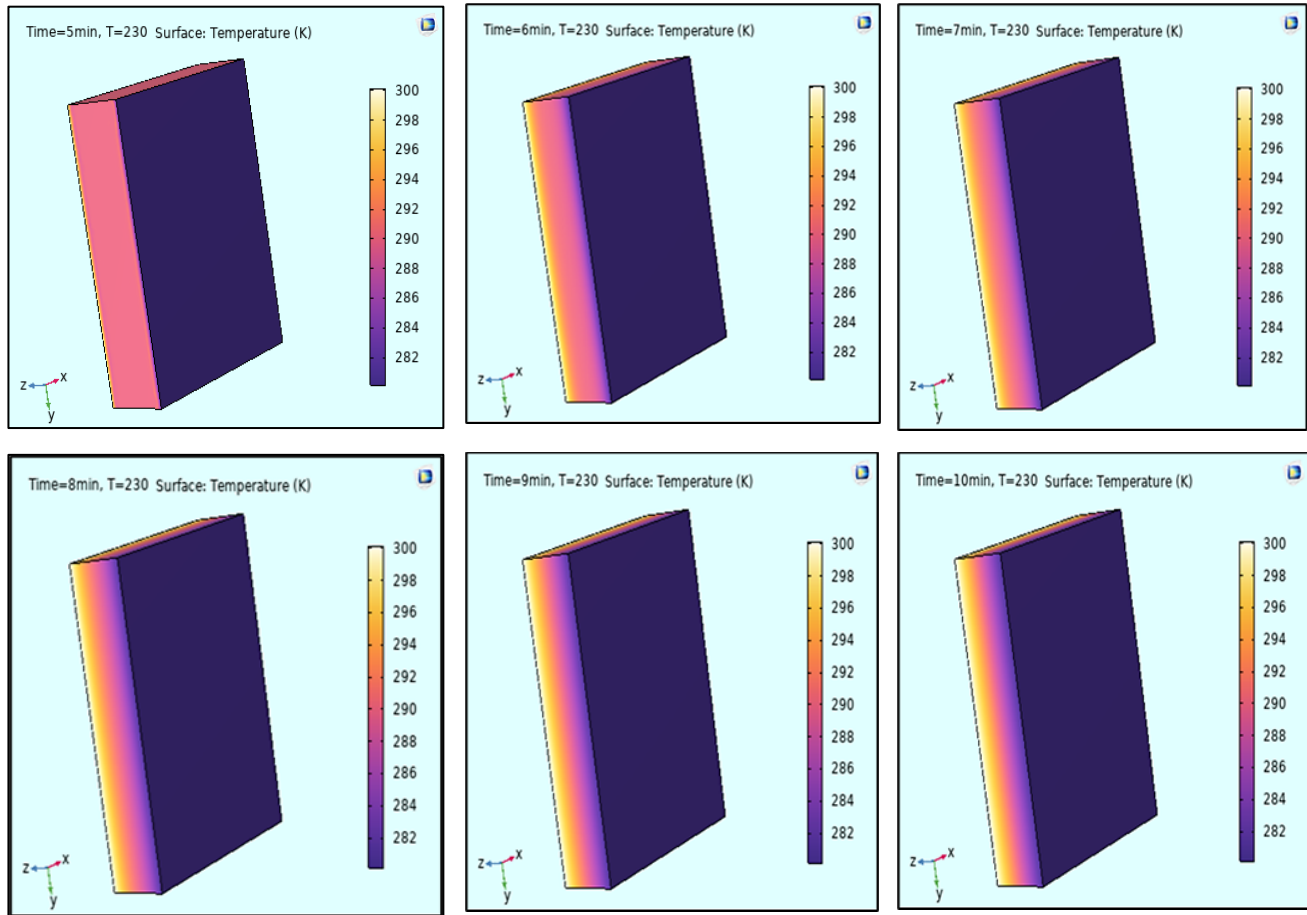


**Figure 3:** Temperature difference of the briquette at  $t = 5$  to 10 minutes

Figure 4 illustrates the isothermal contour of the briquette layer temperature distributions at the x- and y-axis centers during chain-boiler combustion. Initially, the high-temperature zone within the material layer was relatively thin and had lower temperatures than the combustion zone's interior. However, following volatile combustion, the high-temperature zone within the fuel material layer expanded to occupy three-quarters of its thickness, with temperatures gradually decreasing from top to bottom for both the material layer and the gas. This high-temperature zone played a significant role in the fixed carbon combustion process, constituting half of it, while temperatures within the material layer gradually decreased from top to bottom. As ash production occurred, the upper high-temperature region of the material layer steadily diminished, and temperatures within the layer eventually decreased.

Figure 5 displays the average temperature changes of the briquette. Evidently, temperatures progressively increased from the ignition point ( $t=0$  seconds) until  $t = 600$  seconds when the single-pellet biomass was fully ignited. This temperature rise occurred in three phases, starting with endothermic water evaporation, then exothermic separation and combustion of volatiles, and concluding with releasing a substantial amount of heat during coke combustion as the pellets' temperature increased. Finally, air was introduced from top to bottom, resulting in the cooling of the briquette.

In contrast to empirical data, the simulations indicated that the igniting front would extinguish earlier. Figure 6 compares the maximum temperatures attained by the models and the experimental data [27]. While the experimental setup allowed for measuring the entire bed height, estimating the positions of the drying and devolatilization fronts remained essential. The devolatilization front was assumed to be situated at 325 K, and the drying front was estimated to occur within the range of 303K to 310 K. Consequently, each thermocouple records the moments when specific fronts pass through it. This enables the determination of the thickness of each front by multiplying the ignition rate by the time elapsed between the commencement and conclusion of drying or devolatilization. The difference between the overall bed height and the location of the thermocouple measuring the temperature, considered the end of devolatilization, is utilized to gauge the thickness of the char reaction

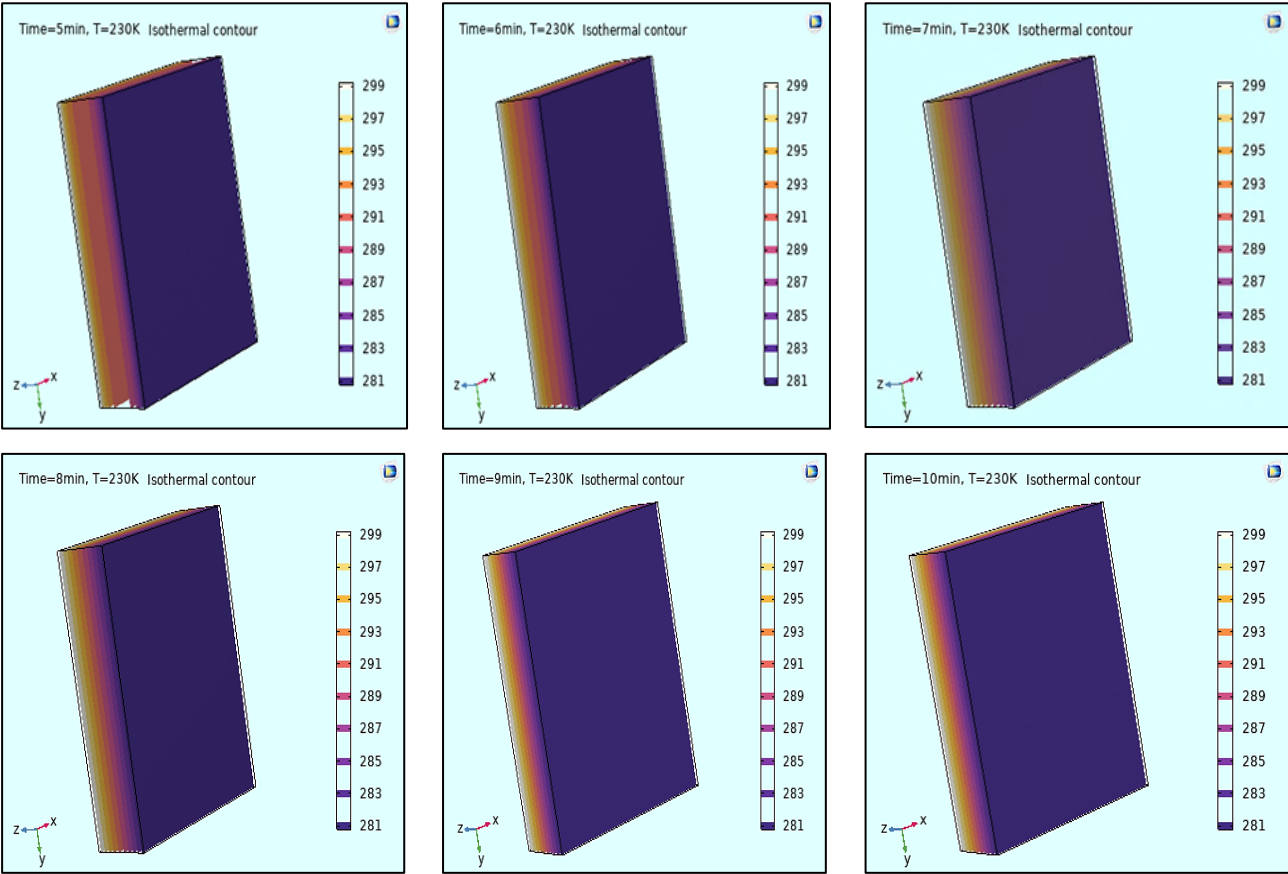


Figure 4: The isothermal contour of the briquette layer temperature distributions at t = 5-10 minutes

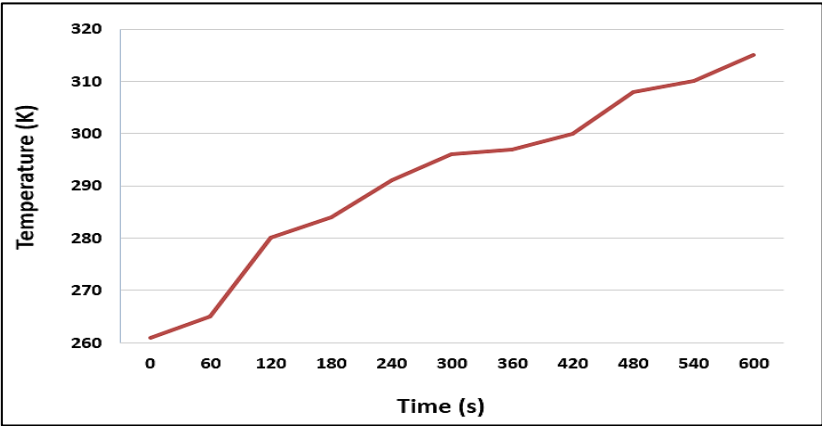


Figure 5: Average briquette temperature changes with time

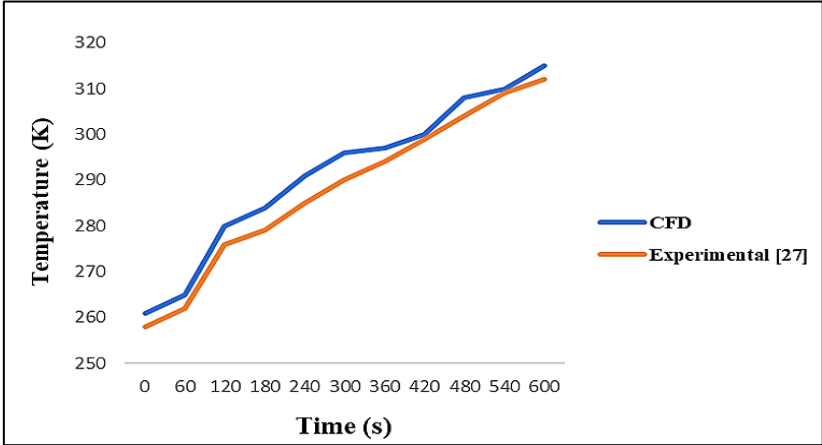


Figure 6: Result validation with experimental approach

## 4. Conclusion

In conclusion, the study employing computer simulations has facilitated a comprehensive understanding of the combustion dynamics of briquettes. The simulation model employed has exhibited high accuracy in predicting the mass loss rate during the combustion process, establishing its utility as a valuable tool for in-depth analysis. Furthermore, our findings underscore that the duration required for the complete combustion of various briquette types is contingent upon their initial moisture content, size, and density. This timeframe typically falls within 5 to 10 minutes, aligning closely with our expectations and experimental observations.

As the combustion progresses, the briquettes undergo temperature elevation and emit gases, including carbon dioxide ( $\text{CO}_2$ ), carbon monoxide ( $\text{CO}$ ), and water ( $\text{H}_2\text{O}$ ). Our simulation revealed a multi-stage process, commencing with the rapid evaporation of water from the briquettes, typically occurring within the initial 5 minutes. Subsequently, as the temperature continues to rise, there is a substantial increase in the production of  $\text{CO}_2$  and  $\text{H}_2\text{O}$ . This phenomenon is primarily attributed to releasing flammable, volatile gases from the briquette's surface, which subsequently react with the oxygen in the surrounding air. This particular stage holds paramount significance in comprehending the intricacies of briquette combustion.

In summary, the computer simulation model has significantly enhanced our grasp of the combustion process of briquettes. It has demonstrated its reliability in predicting their behavior and has emphasized the critical role of initial conditions, such as moisture and size, in the combustion process. This research constitutes a significant step toward optimizing briquettes as an efficient and environmentally friendly energy source, aligning seamlessly with our aspirations for a cleaner and more sustainable energy future.

## Nomenclature

$Q_c$	Gross heat of combustion
$T$	Temperature rise
$E$	Electrical of the calorimeter employed.
$e$	Heat generated
$\rho$	Flow Density
$t$	Time
$x_j - j$	Dimensional coordinate
$u_{g,j}$	Velocity vector
$H$	Total heat enthalpy of the fluid
$S_h$	heat source and radiation heat transfer inside
$u_j$	Velocity vector along the $j$ direction
$r_h$	Heat transfer coefficient.
$d\rho$	Fluid pressure;
$r_i$	the component's mass transfer efficiency $i$ ;
$Y_i$	the mass fraction of component $i$ ;
$R_i$	The generation rate of component $i$ ,
$S_i$	item sources of the production rate.
$Nu$	Nusselt Number
$Sh$	Sherwood Number
$\psi$	Sphericity
$Y$	Inertial loss
$\eta$	permeability
$d_{eq}$	Equivalent diameter
$A_v$	Area Volume Ratio
$h$	Convection coefficient
$D_{cil}$	Cylindrical diameter
$G_s$	Heat conductance through a particle
$G_c$	Heat conductance through the contact between particles

## Acknowledgment

This research was a labor of love, made possible by the hard work and dedication of the authors, as well as the support of our friends and families. We would like to express our gratitude to everyone who made this research possible, including those who provided encouragement and support.

## Author contributions

Conceptualization, T. Adeyi; methodology, T. Adeyi; validation, S. Ekun; investigation, O. Alabi; writing—original draft preparation, O. Alabi; writing—review and editing, O. Alabi, T. Adeyi and S. Ekun;; visualization, T. Adeyi and S. Ekun; supervision, S. Ekun. All authors have read and agreed to the published version of the manuscript.



## Funding

This research received no specific grant from any funding agency in the public, commercial, or not-for-profit sectors.

## Data availability statement

The data that support the findings of this study are available on request from the corresponding author.

## Conflicts of interest

The authors declare that they have no conflicts of interest concerning the publication of this paper.

## References

- [1] R. B. W. Evaristo, N. A. Viana, M. G. Guimarães, A. T. do Vale, J. L. de Macedo, and G. F. Ghesti, Evaluation of waste biomass gasification for local community development in central region of Brazil, *Biomass Convers. Biorefinery*, 12 (2022) 2823–2834. <http://dx.doi.org/10.1007/s13399-020-00821-y>
- [2] H. Gilvari, W. de Jong, and D. L. Schott, Quality parameters relevant for densification of bio-materials: Measuring methods and affecting factors - A review, *Biomass Bioenergy*, 120 (2019) 117–134. <http://dx.doi.org/10.1016/j.biombioe.2018.11.013>
- [3] T. Huggins, H. Wang, J. Kearns, P. Jenkins, and Z. J. Ren, Biochar as a sustainable electrode material for electricity production in microbial fuel cells, *Bioresour. Technol.*, 157 (2014) 114–119. <http://dx.doi.org/10.1016/j.biortech.2014.01.058>
- [4] A. O. Adeaga, O. O. Alabi, and S. A. Akintola, Experimental investigation of the potential of liquified petroleum gas in vapour compression refrigeration system, *LAUTECH J. Eng. Technol.*, 17 (2003) 1–7.
- [5] R. Picchio, R. Venanzi, W. Stefanoni, A. Suardi, D. Tocci and L. Pari, Pellet production from woody and non-woody feedstocks : A review on biomass quality evaluation, *Energies*, 13 (2020) 1–20. <https://doi.org/10.3390/en13112937>
- [6] O. O. Alabi, G. O. Ogunsiji, and S. A. Dada, Performances Evaluation of Blended Alternative Refrigerant In Vapour Compression Refrigeration System, *FUW Trends Sci. Technol. J.*, 8 (2023) 228–234.
- [7] M. Jewiarz, M. Wróbel, K. Mudryk, and S. Szufa, Impact of the drying temperature and grinding technique on biomass grindability, *Energies*, 13(2020). <http://dx.doi.org/10.3390/en13133392>.
- [8] R. Chen et al., Numerical Simulation of Bed Combustion in Biomass-Briquette Boiler, *J. Energy Eng.*, 146 (2020) 1–11. [https://doi.org/10.1061/\(ASCE\)EY.1943-7897.0000653](https://doi.org/10.1061/(ASCE)EY.1943-7897.0000653)
- [9] A. Boldrin et al., Optimised biogas production from the co-digestion of sugar beet with pig slurry: Integrating energy, GHG and economic accounting, *Energy*, 112 (2016) 606–617. <http://dx.doi.org/10.1016/j.energy.2016.06.068>
- [10] B. Singh, A. Guldhe, I. Rawat, and F. Bux, Towards a sustainable approach for development of biodiesel from plant and microalgae, *Renew. Sustain. Energy Rev.*, 29 (2014) 216–245. <http://dx.doi.org/10.1016/j.rser.2013.08.067>
- [11] H. Chyuan, W. Chen, A. Farooq, Y. Yang, and K. Teong, Catalytic thermochemical conversion of biomass for biofuel production : A comprehensive review, *Renew. Sustain. Energy Rev.*, 113 (2019) 109266. <http://dx.doi.org/10.1016/j.rser.2019.109266>
- [12] M. A. Gómez, J. Porteiro, D. Patiño, and J. L. Míguez, CFD modelling of thermal conversion and packed bed compaction in biomass combustion, *Fuel*, 117 (2014) 716–732. <http://dx.doi.org/10.1016/j.fuel.2013.08.078>
- [13] R. Chen, Y. Ai, T. Zhang, Y. Rao, H. Yue, and J. Zheng, Numerical Simulation of Biomass Pellet Combustion Process, *Int. J. Heat Technol.*, 37 (2019) 1107–1116.
- [14] O. O. Alabi, O. A. Adeaga, and S. A. Akintola, Numerical Modeling and Investigation of Flow of Incompressible Non-Newtonian Fluids through Uniform Slightly Deformable Channel, *2023 Int. Conf. Sci. Eng. Bus. Sustain. Dev. Goals*, 1 (2020) 1–6. <http://dx.doi.org/10.1109/SEB-SDG57117.2023.10124471>
- [15] M. H. Rahdar et al., A Review of Numerical Modeling and Experimental Analysis of Combustion in Moving Grate Biomass Combustors, *Energy Fuels*, 33 (2019) 9367–9402. <http://dx.doi.org/10.1021/acs.energyfuels.9b02073>
- [16] R. Karim and J. Naser, CFD modelling of combustion and associated emission of wet woody biomass in a 4 MW moving grate boiler, *Fuel*, 222 (2018) 656–674. <http://dx.doi.org/10.1016/j.fuel.2018.02.195>
- [17] R. Mehrabian et al., A CFD model for thermal conversion of thermally thick biomass particles, *Fuel Process. Technol.*, 95 (2020) 96–108. <http://dx.doi.org/10.1016/j.fuproc.2011.11.021>
- [18] P. Pradhan, A. Arora, and S. M. Mahajani, Pilot scale evaluation of fuel pellets production from garden waste biomass, *Energy Sustain. Dev.*, 43 (2018) 1–14. <http://dx.doi.org/10.1016/j.esd.2017.11.005>

- [19] J. Porteiro, J. Collazo, D. Patin, E. Granada, and J. C. Moran, Numerical Modeling of a Biomass Pellet Domestic Boiler, *Energy Fuels*, 23 (2009) 2043–2051. <https://doi.org/10.1021/ef8008458>
- [20] B. N. Madanayake, S. Gan, C. Eastwick, and H. K. Ng, Biomass as an energy source in coal co-firing and its feasibility enhancement via pre-treatment techniques, *Fuel Process. Technol.*, 159 (2017) 287–305. <http://dx.doi.org/10.1016/j.fuproc.2017.01.029>
- [21] E. Granada and J. C. Moran, Mathematical modelling of the combustion of a single wood particle, *Fuel Process. Technol.*, 87 (2006) 169–175. <http://dx.doi.org/10.1016/j.fuproc.2005.08.012>
- [22] J. You, X. A. Walter, J. Greenman, C. Melhuish, and I. Ieropoulos, Stability and reliability of anodic biofilms under different feedstock conditions: Towards microbial fuel cell sensors, *Sens. Bio-Sensing Res.*, 6 (2015) 43–50. <http://dx.doi.org/10.1016/j.sbsr.2015.11.007>
- [23] Y. Yao, C. Ramu, A. Procher, J. Littlejohns, J. M. Hill, and J. W. Butler, Potential for Thermo-Chemical Conversion of Solid Waste in Canada to Fuel, Heat, and Electricity, *Waste*, 1 (2023) 689–710. <https://doi.org/10.3390/waste1030041>
- [24] E. Carter et al., Development of renewable, densified biomass for household energy in China, *Energy Sustain. Dev.*, 46 (2018) 42–52. <http://dx.doi.org/10.1016/j.esd.2018.06.004>
- [25] M. Elkelawy, H. Alm-Eldin Bastawissi, E. A. El Shenawy, M. Taha, H. Panchal, and K. K. Sadasivuni, Study of performance, combustion, and emissions parameters of DI-diesel engine fueled with algae biodiesel/diesel/n-pentane blends, *Energy Convers. Manage.*, 210 (2021) 100058. <http://dx.doi.org/10.1016/j.ecmx.2020.100058>
- [26] H. Weldekidan, V. Strezov, J. He, R. Kumar, S. Asumadu-Sarkodie, I. N. Y. Doyi, S. Jahan, T. Kan and Graham, Town Energy conversion efficiency of pyrolysis of chicken litter and rice husk biomass, *Energy Fuels*, 33 (2019) 6509–6514. <https://doi.org/10.1021/acs.energyfuels.9b01264>
- [27] O. A. Sotannde, A. O. Oluyeye, and G. B. Abah, Physical and combustion properties of charcoal briquettes from neem wood residues, *Int. Agrophys.*, 24 (2010) 189–194.